Intersystem Crossing Observed by Ultrasonic Relaxation of the Singlet–Quintet Spin Equilibrium of Iron(II) Complexes in Solution

James K. Beattie,* Robert A. Binstead, and Robert J. West†

Contribution from the School of Chemistry, The University of Sydney, Sidney, N.S.W. 2006, Australia. *Received September 20, 1977*

Abstract: Resonance and pulsed ultrasonic techniques have been used to determine relaxation times for the spin equilibrium of tetrahydrofuran solutions of bis(hydrotris(pyrazolyl)borato)iron(II), $Fe(HB(pz)_3)_2$, and of aqueous solutions of bis(2-(2-pyridylamino)-4-(2-pyridyl)thiazole)iron(II) chloride dihydrate, $[Fe(papth)_2]Cl_2 \cdot 2H_2O$. Relaxation times at 25 °C for the two complexes are 33.0 ± 0.7 and 41.00 ± 0.14 ns, respectively. From the relaxation amplitudes the high-spin states were found to be 22 ± 1 and 11.0 ± 0.3 $cm^3\ mol^{-1}$ larger than their respective low-spin states. The temperature dependence of the relaxation times and the equilibrium constants measured by the Evans' NMR method imply activation enthalpies for the singlet-quintet interconversion of $\Delta H^{\ddagger}_{15} = 5.64 \pm 0.13$ and $\Delta H^{\ddagger}_{51} = 0.62 \pm 0.13$ kcal mol^{-1} for $Fe(HB(pz)_3)_2$ and $\Delta H^{\ddagger}_{15} = 7.63 \pm 0.25$ and $\Delta H^{\ddagger}_{51} = 3.72 \pm 0.25$ kcal mol^{-1} for $Fe(papth)_2^{2+}$. Using absolute rate theory the transmission coefficients, κ, are calculated to be $\geq 10^{-4.2}$ and $\geq 10^{-2.52}$, respectively, for these spin-forbidden $\Delta S = 2$ intersystem crossing processes.

Introduction

The relaxation of the thermal equilibrium between two states of different spin multiplicities in a metal complex can be described as an intersystem crossing process.[1,2] These equilibria provide a convenient means of investigating the dynamics of intersystem crossing which are otherwise only accessible in excited states. They are of further interest as examples of unimolecular electronic isomerizations, and their kinetics are important for understanding those electron transfer reactions which are accompanied by changes in spin multiplicity.

Although there have been many magnetic and spectroscopic studies of such spin equilibria, in most cases these have been performed on solid state samples. There is evidence[3] that some of the properties observed are influenced by lattice effects and, particularly, that the dynamic properties observed are not those of the independent molecules. For these reasons we have pursued the investigation of the dynamics of spin equilibria in metal complexes with solution studies.

Using the laser temperature-jump technique we have previously measured the rate of intersystem crossing between the ^1A and ^5A states of bis(hydrotris(pyrazolyl)borato)iron(II), $Fe(HB(pz)_3)_2$ (I).[4]

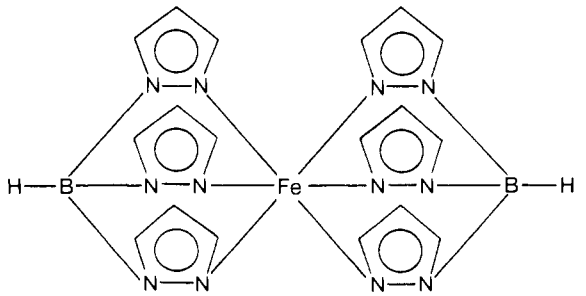

(I)

A relaxation time of 32 ± 10 ns was observed at 25 °C using CH_2Cl_2–CH_3OH solutions. Subsequently, similar studies using other iron(II) and iron(III) spin equilibrium complexes have been performed using the same apparatus with observed relaxation times ranging from 135 ns to the 20–30-ns limit of the method.[5]

† Deceased.

In order to obtain more accurate results, to extend the time range of the observations to observe faster reactions, and, in particular, to determine the activation parameters for the intersystem crossing process, we have applied ultrasonic relaxation techniques to these equilibria. We now report our observations of ultrasonic relaxations ascribed to the spin equilibria in solutions (eq 1) of $Fe(HB(pz)_3)_2$ and of bis(2-(2-pyridylamino)-4-(2-pyridyl)thiazole)iron(II) chloride dihydrate, $[Fe(papth)_2]Cl_2 \cdot 2H_2O$ (II).

$$\text{singlet} \underset{k_{51}}{\overset{k_{15}}{\rightleftharpoons}} \text{quintet} \qquad (1)$$

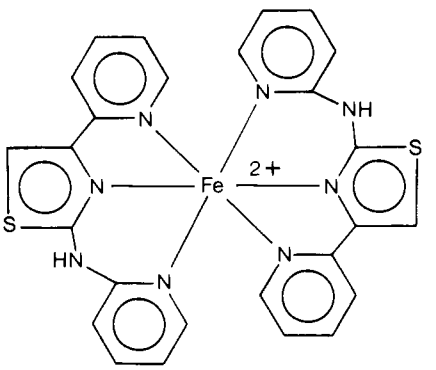

(II)

From the temperature dependence of the relaxation times we can assess the barrier to the intersystem crossing and can calculate lower limits of the transmission coefficients for the probability of the spin-forbidden intersystem crossing in these octahedral metal complexes.

Experimental Section

Materials. The complex $Fe(HB(pz)_3)_2$ was prepared as described in the literature.[6] The complex was purified by chromatography on activated alumina in CH_2Cl_2 (Merck UVASOL) under argon, recrystallized from toluene, and characterized by elemental analyses. Anal. Calcd for $C_{18}H_{20}N_{12}B_2Fe$: C, 44.86; H, 4.18; N, 34.88; B, 4.49; Fe, 11.59. Found: C, 45.10; H, 4.17; N, 34.79; B, 4.38; Fe, 11.20. Merck UVASOL THF was used as the solvent for the ultrasonics experiments without further purification.

The complex $[Fe(papth)_2]Cl_2 \cdot 2H_2O$ was supplied by Professor H. A. Goodwin, U.N.S.W., Sydney, Australia. The complex was recrystallized from distilled water before use and characterized by el-

0002-7863/78/1500-3044$01.00/0

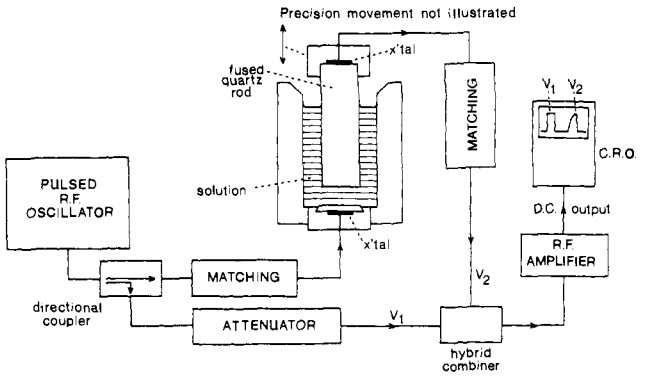

Figure 1. Schematic diagram of the pulsed ultrasonic absorption apparatus.

emental analyses. Distilled water was used for the ultrasonics experiments. Anal. Calcd for $C_{26}H_{24}N_8O_2S_2Cl_2Fe$: C, 46.51; H, 3.60; N, 16.69; O, 4.77; S, 9.55; Cl, 10.56; Fe, 8.32. Found: C, 46.29; H, 3.44; N, 16.78; S, 9.24; Cl, 10.45; Fe, 8.08. Microanalyses were performed by Alfred Bernhardt Microanalytical Laboratories, West Germany.

Methods. Solution magnetic moments of 0.05 M $Fe(HB(pz)_3)_2$ in THF and of 0.02 M $[Fe(papth)_2]Cl_2 \cdot 2H_2O$ in H_2O were measured using the Evans ^1H NMR method at 90 MHz (Bruker HX-90).[7] Internal references of 4% v/v Me_4Si and 3% *t*-BuOH were used, respectively. Probe temperatures were measured with internal capillaries of methanol (Merck AR)[8] and ethylene glycol (Merck AR).[9] The validity of these literature temperature calibrations was checked against the melting points of several pure organic liquids and solids. The data were corrected for changes of solvent density and hence for sample concentration with temperature.

Ultrasonic absorption measurements were collected in the frequency range 1-100 MHz. Measurements between 1 and 36 MHz were made with swept frequency acoustic resonance cells based on the designs of Eggers[10] and Labhardt and Schwarz.[11] These cells use 25.4-mm diameter 5-MHz overtone-type quartz crystals supplied by Valpey-Fisher, Hopkinton, Mass. The crystals were selected for optical flatness using a Fabry-Perot interferometer.[12] For 0.05 M solutions of $Fe(HB(pz)_3)_2$ in THF the Eggers' type cell was used owing to the need for complete solvent inertness. In this cell the transducers are mechanically clamped against a PTFE sealing washer over a machined edge of the stainless steel mountings. The mechanical clamping has an adverse effect on the performance of the cell but with careful mounting of the transducers acceptable performance can be obtained. Measurements were not made above 15 MHz owing to the high solvent absorption.

For 0.02 M solutions of $Fe(papth)_2^{2+}$ the Labhardt and Schwarz[11] type cell was used. In this cell the transducers are held in their stainless steel mountings with various types of silicone rubber glue,[13] and are therefore under no mechanical stress. As the transducers remain optically flat the performance is much improved over the clamped type of cell.

In both cases a Wandel and Goltermann (Reutlingen, West Germany) PSM-5 level measuring set with a Hewlett-Packard 5382A frequency counter was used to measure the 3-dB bandwidths and frequencies of the resonances. Temperatures were controlled to within ±0.005 °C using a Bayley Instruments Co. (Danville, Calif.) Model 121 precision temperature controller operating the 500-W heater of the water bath in which the resonance cell was submerged. Cooling was accomplished by cirulating fluid from a Colora WK5 refrigerated bath through a cooling coil in the main bath at 1-4 °C lower than the desired main bath temperature.

Between 7.5 and 100 MHz measurements were made with a pulsed ultrasonic cell of our design based on principles described in the literature.[14] This instrument uses 17.5-mm diameter 2.5- and 5-MHz overtone type quartz crystals supplied by Valpey-Fisher. For 0.05 M solutions of $Fe(HB(pz)_3)_2$ in THF, measurements were made between 7.5 and 50 MHz using electronics including the Arenberg Ultrasonics Inc. (Jamaica Plain, Mass.) pulsed oscillator PG-650C, wide band amplifier WA-600E, preamplifier PA-620B, and precision attenuator ATT-693. For 0.02 M solutions of $Fe(papth)_2^{2+}$ in H_2O, measurements were made between 7.5 and 100 MHz using new Arenberg

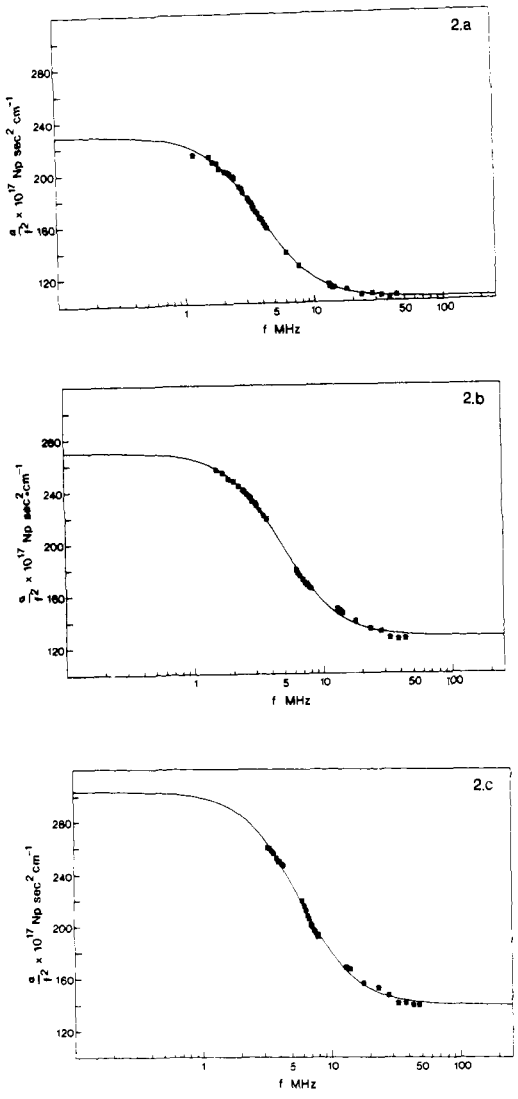

Figure 2. The ultrasonic absorption of 0.05 M solutions of $Fe(HB(pz)_3)_2$ in THF at (a) 5 °C, (b) 25 °C, and (c) 40 °C.

electronics including the pulsed oscillator PG-653C, wide band amplifier WA-600E-DC5, preamplifier PA-620B, VHF receiver VR-720, and precision attenuator ATT-650 (Figure 1). In addition a Kay Elemetrics (Pine Brook, N.J.) 1/432D 0.1 dB step attenuator was employed when small attenuation increments were required.

In both cases frequency calibration was accomplished using the zero beat frequency technique with a Hewlett-Packard 3200B VHF oscillator, 3320A frequency synthesizer, and 5382A frequency counter. Signal splitting and combining was accomplished using the Wide Band Engineering (Phoenix, Ariz.) A73 directional coupler and A66-GA precision hybrid combiner. Temperatures were controlled to within ±0.005 °C using the precision bath described above.

The pulsed cell has been tested, using liquids of known constant absorption, in the frequency range 7.5-100 MHz. Plots of attenuation vs. path length are linear and were refined by linear least-squares regression. In each case the measured absorption (α/f^2) is flat and agrees with the literature values; e.g., for H_2O[15] at 25 °C, $(21.3 \pm 0.3) \times 10^{-17}$ Np s^2 cm^{-1}; for dried THF[16] at 20 °C, $(126 \pm 3) \times 10^{-17}$ Np s^2 cm^{-1}; and for MeOH[17] at 25 °C, $(30.5 \pm 0.5) \times 10^{-17}$ Np s^2 cm^{-1}.

Results

Solutions of both iron(II) complexes display single ultrasonic relaxation processes. The ultrasonic absorption curves for 0.05 M solutions of $Fe(HB(pz)_3)_2$ in THF are shown in Figure 2 and for 0.018 M solutions of $Fe(papth)_2^{2+}$ in H_2O in Figure 3. The absorbance curves were fitted by nonlinear least-squares analysis to eq 2, representing a single relaxation process.[18]

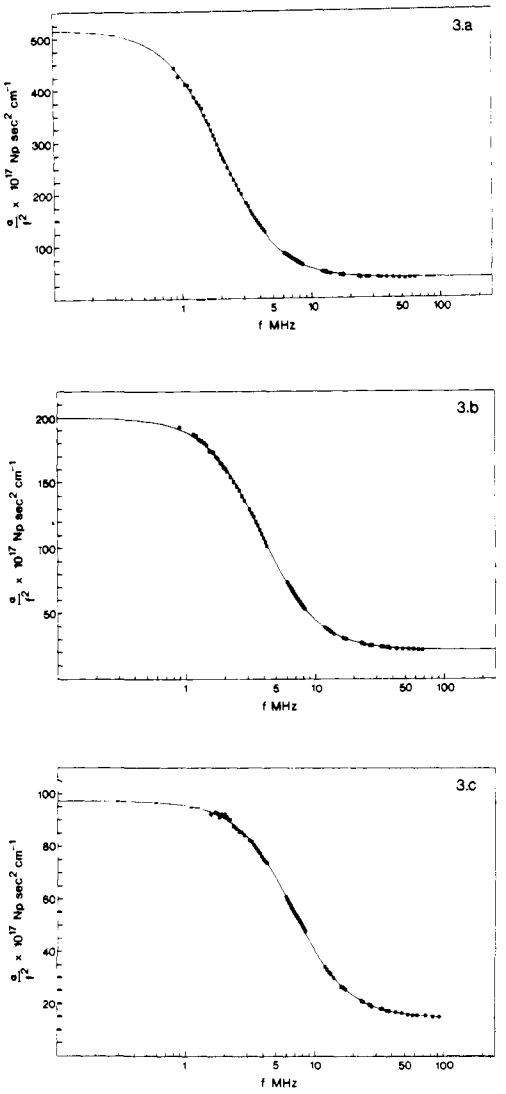

Figure 3. The ultrasonic absorption of 0.02 M solutions of $[Fe(papth)_2]Cl_2 \cdot 2H_2O$ in H_2O at (a) 10 °C, (b) 25 °C, and (c) 40 °C.

Values of the parameters A, B, and τ so obtained are given in Tables I and II,

$$\alpha/f^2 = A(1 + \omega^2\tau^2)^{-1} + B \qquad (2)$$

where α is the absorption coefficient (Np cm^{-1}); f is the frequency (Hz); ω is the angular frequency (rad s^{-1}) = $2\pi f$; τ is the relaxation time (s); and A and B are constants for a particular relaxation curve. The relaxation times were found to be concentration independent and the relaxation amplitudes, A, to depend linearly on concentration (Tables I and II), as expected for relaxations due to unimolecular processes.

To interpret these results it is necessary to know the equilibrium constants and the thermodynamic parameters for equilibrium 1 under the conditions of the experiment. Consequently, the effective magnetic moments of solutions of the complexes were measured using the Evans' NMR method.[7] For $Fe(HB(pz)_3)_2$ measurements were made in THF between −50 and 50 °C. The data are listed in Table III and the effective magnetic moments at the temperatures of the ultrasonic experiments are given in Table I. The value of 2.30 μ_B at 25 °C in THF can be compared with 2.71 μ_B found in CH_2Cl_2.[19] To calculate the equilibrium constant the magnetic moment of the high-spin state was taken as 5.22 μ_B.[19] A value of 1.0 μ_B for the magnetic moment of the low-spin state was required to obtain a linear plot of ln K against T^{-1} (Figure 4). Such a value is common for the low-spin limit of iron(II) spin-equilibrium complexes.[20] From the temperature dependence of the equilibrium constant the enthalpy difference between the two states is calculated to be 5.03 ± 0.07 kcal mol^{-1}, compared with 3.85 kcal mol^{-1} found in CH_2Cl_2 solution,[19] and the entropy difference is 13.6 ± 0.2 cal deg^{-1} mol^{-1} compared with 11.4 cal deg^{-1} mol^{-1}.

For $Fe(papth)_2^{2+}$ measurements were made in H_2O be-

Table I. Collected Data and Results for $Fe(HB(pz)_3)_2$[a]

	5 °C	25 °C	40 °C
$A \times 10^{17}$, Np s^2 cm^{-1}	126.6 ± 1.1	141.9 ± 1.6[d]	163 ± 3
$B \times 10^{17}$, Np s^2 cm^{-1}	102.7 ± 0.5	127.9 ± 0.8[d]	140 ± 1
τ, ns	41.7 ± 0.6	33.0 ± 0.7[d]	28.0 ± 0.5
μ_{eff}, μ_B[b]	1.87	2.30	2.63
K_{15}	0.106	0.195	0.292
$\Delta H°$, kcal mol^{-1}		5.03 ± 0.07	
$\Delta S°$, cal deg^{-1} mol^{-1}		13.6 ± 0.2	
C_{total}, M	0.0528	0.05164[d]	0.0513
$\Gamma \times 10^3$, M	4.57	7.04	8.98
ρ, g cm^{-3}[c]	0.9021	0.8819	0.8668
v, cm s^{-1}[c]	136300	126900	120500
$\alpha_P/\rho C_p$, cm^3 kcal^{-1}[c]	2.6478	2.7705	2.8679
$\Delta V°$, cm^3 mol^{-1}	21.3	22.2	23.5
k_{15}, s^{-1}	2.30×10^6	4.93×10^6	8.08×10^6
k_{51}, s^{-1}	2.17×10^7	2.53×10^7	2.76×10^7
$\Delta G^{\ddagger}_{15}$, kcal mol^{-1}		8.33 ± 0.18	
$\Delta G^{\ddagger}_{51}$, kcal mol^{-1}		7.36 ± 0.18	
$\Delta H^{\ddagger}_{15}$, kcal mol^{-1}		5.64 ± 0.13	
$\Delta H^{\ddagger}_{51}$, kcal mol^{-1}		0.62 ± 0.13	
$\Delta S^{\ddagger}_{15}$, cal deg^{-1} mol^{-1}		−9.0 ± 0.4	
$\Delta S^{\ddagger}_{51}$, cal deg^{-1} mol^{-1}		22.6 ± 0.4	

[a] The quoted error bars are for one standard deviation. [b] The estimated error is ± 0.03 μ_B. [c] Pure solvent values were assumed for the physical constants. [d] At 0.0139 M, A = (38.4 ± 0.8) × 10^{-17} Np s^2 cm^{-1}, B = (127.8 ± 0.4) × 10^{-17} Np s^2 cm^{-1}, τ = (30.9 ± 1.3) ns.

Table II. Collected Data and Results for $Fe(papth)_2^{2+}$[a]

	10 °C	25 °C	40 °C
$A \times 10^{17}$, Np s^2 cm^{-1}	478.0 ± 1.9	177.5 ± 0.4[d]	82.47 ± 0.21
$B \times 10^{17}$, Np s^2 cm^{-1}	38.15 ± 0.43	22.40 ± 0.16[d]	14.81 ± 0.12
τ, ns	78.29 ± 0.42	41.00 ± 0.14[d]	23.65 ± 0.10
μ_{eff}, μ_B[b]	4.58	4.86	5.07
K_{15}	1.66	2.36	3.24
$\Delta H°$, kcal mol^{-1}		3.91 ± 0.10	
$\Delta S°$, cal deg^{-1} mol^{-1}		14.8 ± 0.3	
C_{total}, M	0.01857	0.01850[d]	0.01792
$\Gamma \times 10^3$, M	4.36	3.87	3.23
ρ, g cm^{-3}[c]	0.99973	0.99707	0.99224
v, cm s^{-1}[c]	146 100	149 700	153 300
$\alpha_p/\rho C_P$, cm^3 kcal^{-1}[c]	0.08781	0.25825	0.38914
$\Delta V°$, cm^3 mol^{-1}	11.04	10.71	11.19
k_{15}, s^{-1}	7.98×10^6	1.69×10^7	3.23×10^7
k_{51}, s^{-1}	4.80×10^6	7.17×10^6	9.98×10^6
$\Delta G^{\ddagger}_{15}$, kcal mol^{-1}		7.60 ± 0.35	
$\Delta G^{\ddagger}_{51}$, kcal mol^{-1}		8.11 ± 0.35	
$\Delta H^{\ddagger}_{15}$, kcal mol^{-1}		7.63 ± 0.25	
$\Delta H^{\ddagger}_{51}$, kcal mol^{-1}		3.72 ± 0.25	
$\Delta S^{\ddagger}_{15}$, cal deg^{-1} mol^{-1}		0.09 ± 0.8	
$\Delta S^{\ddagger}_{51}$, cal deg^{-1} mol^{-1}		−14.7 ± 0.8	

[a] The quoted error bars are for one standard deviation. [b] The estimated error is ±0.03 μ_B. [c] Pure solvent values were assumed for the physical constants. [d] At 0.00916 M, A = (92.7 ± 0.4) × 10^{-17} Np s^2 cm^{-1}, B = (22.1 ± 0.2) × 10^{-17} Np s^2 cm^{-1}, τ = (42.0 ± 0.3) ns.

Table III. Solution Magnetic Susceptibility Measurements: $Fe(HB(pz)_3)_2$[a]

Δf, Hz MeOH	T, K	Δf, Hz Me_4Si	$\chi_g \times 10^6$,[b] cgs	χ_M^{cor} $\times 10^3$ [c]	μ_{eff},[d] μ_B
199.078	221.2	2.198	1.163	0.701	1.12
191.165	232.9	3.077	1.346	0.790	1.22
183.178	244.3	4.249	1.595	0.910	1.34
174.926	255.7	5.934	1.956	1.084	1.50
165.740	267.9	7.986	2.406	1.300	1.68
157.094	279.0	10.404	2.943	1.559	1.87
148.081	290.0	13.115	3.557	1.853	2.08
138.116	301.7	16.925	4.429	2.276	2.35
126.686	314.3	21.468	5.494	2.789	2.66
115.256	326.2	26.377	6.667	3.354	2.97

[a] $C_{total} = 0.05046$ M in THF at $T = 25.0$ °C. The data were corrected for changes in solvent density with temperature. [b] Includes $\chi_0(THF) = 0.722 \times 10^{-6}$ cgs. [c] Includes $\chi_D = 0.141 \times 10^{-3}$ mol^{-1}, which was obtained using Pascal's constants and constitutive corrections. [d] The estimated error is ± 0.03 μ_B.

Table IV. Solution Magnetic Susceptibility Measurements: $Fe(papth)_2^{2+}$ [a]

Δf, Hz ethylene glycol	T, K	Δf, Hz t-BuOH	$\chi_g \times 10^6$,[b] cgs	χ_M^{cor} $\times 10^3$ [c]	μ_{eff},[d] μ_B
157.283	287.2	31.984	13.79	9.49	4.69
148.888	296.7	32.825	14.16	9.74	4.83
137.622	309.5	33.745	14.59	10.02	5.00
127.645	320.9	34.475	14.96	10.27	5.16
117.375	332.5	34.625	15.10	10.36	5.27
107.252	344.0	34.185	15.01	10.30	5.35
97.422	355.2	33.745	14.92	10.25	5.42

[a] $C_{total} = 0.01930$ M in H_2O at $T = 21.5$ °C. The data were corrected for changes in solvent density with temperature. [b] Includes $\chi_0(H_2O) = 0.718 \times 10^{-6}$ cgs. [c] Includes $\chi_D = 0.2278 \times 10^{-3}$ mol^{-1}, which was obtained using Pascal's constants and constitutive corrections. [d] The estimated error is ± 0.03 μ_B.

tween 15 and 82 °C; the data are given in Table IV. Previous experiments using magnetic susceptibility[21] and Mossbauer techniques[22] have indicated that this complex exhibits a spin equilibrium in the solid state with the magnetic moment strongly dependent on the anion present and on the degree of hydration. In order to fit the equation ln K vs. T^{-1} describing the solution spin equilibrium to the magnetic moment data using linear least squares, a limiting magnetic moment for the high-spin state of 5.8 μ_B was required. This was independent of the value used for the moment of the low-spin state within the range 0.0–1.0 μ_B. Consequently, a value of 0 μ_B was used for the low-spin state. Although the value of 5.8 μ_B is relatively high for an Fe(II) complex, previous work[23] had indicated that certain sets of parameters can produce such a magnetic moment. Using these limiting values a straight line plot of ln K vs. T^{-1} was obtained over the entire temperature range (Figure 5). The effective magnetic moments at the temperatures of the ultrasonics experiments are given in Table II. From the temperature dependence of the equilibrium constant the enthalpy difference between the two states is calculated to be 3.91 ± 0.10 kcal mol^{-1} and the entropy difference 14.8 ± 0.3 cal deg^{-1} mol^{-1}.

Discussion

Solutions of both iron(II) complexes exhibit single ultrasonic relaxations with concentration-independent relaxation times. For $Fe(HB(pz)_3)_2$ in THF at 25 °C the observed relaxation time of 33.0 ± 0.7 ns can be compared with a relaxation time of 32 ± 10 ns observed previously using the laser temperature-jump technique.[4] This relaxation was identified spectroscopically as arising from perturbation of the spin equilibrium. The ultrasonic relaxation can therefore be ascribed to a unimolecular isomerization of the iron(II) complex between two states of different spin multiplicities. For the $Fe(papth)_2^{2+}$ complex a relaxation time of 41.00 ± 0.14 ns is obtained at 25 °C which is similarly concentration independent and can be assumed to arise from a unimolecular process. Since magnetic moment measurements indicate that the $Fe(papth)_2^{2+}$ complex exhibits a spin equilibrium in solution and since the amplitude of the ultrasonic relaxation displays a temperature dependence consistent with the temperature dependence of the spin equilibrium, we similarly identify the ultrasonic relaxation as due to perturbation of this spin equilibrium.

A measure of the volume difference between the singlet and quintet isomers can be obtained from the magnitude of the ultrasonics absorption. Equation 2 can be written as

$$\alpha/f^2 = \frac{2\pi^2\rho v}{RT}\left(\Delta V^\circ - \frac{\alpha_P}{\rho C_p}\Delta H^\circ\right)^2 \frac{\Gamma\tau}{1+\omega^2\tau^2} + B \quad (3)$$

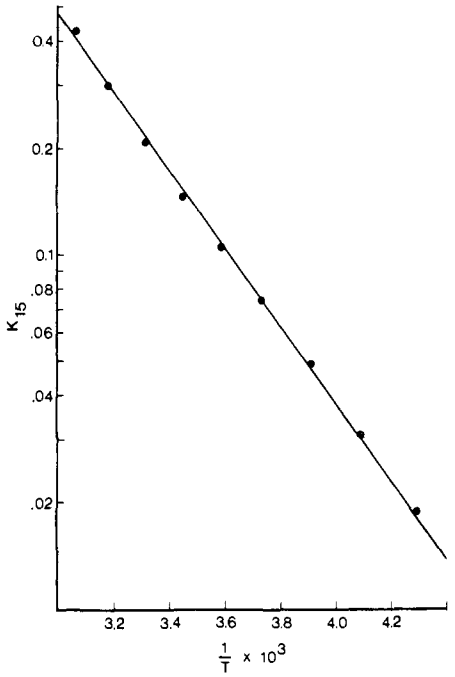

Figure 4. The temperature dependence of the equilibrium constant for $Fe(HB(pz)_3)_2$ in THF.

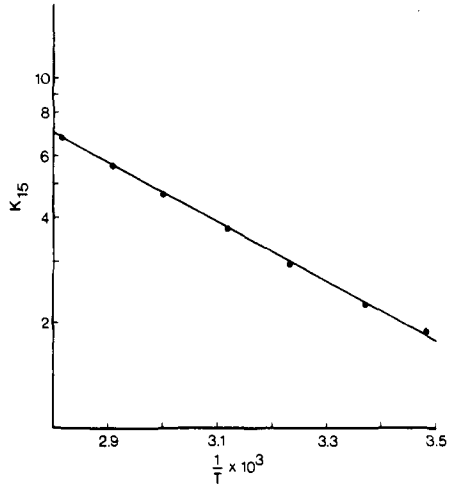

Figure 5. The temperature dependence of the equilibrium constant for $Fe(papth)_2^{2+}$ in H_2O.

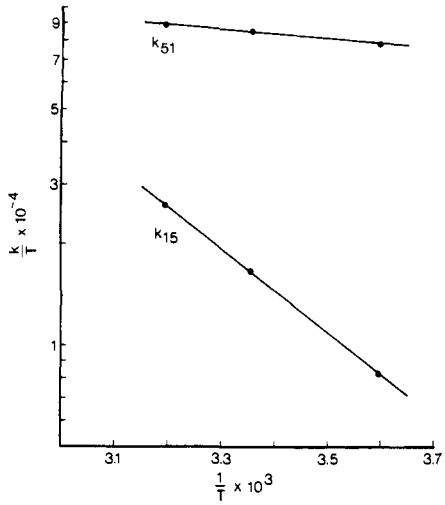

Figure 6. Eyring plots of the temperature dependence of the rate constants k_{15} and k_{51} for the $Fe(HB(pz)_3)_2$ system.

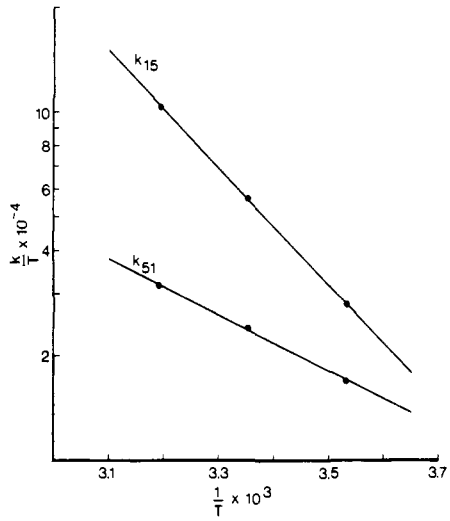

Figure 7. Eyring plots of the temperature dependence of the rate constants k_{15} and k_{51} for the $Fe(papth)_2^{2+}$ system.

Hence the excess absorption due to the chemical relaxation for $\omega \ll \tau$ is given by

$$A = \frac{2\pi^2\rho v}{RT}\left(\Delta V^\circ - \frac{\alpha_P}{\rho C_p}\Delta H^\circ\right)^2 \Gamma\tau \qquad (4)$$

where ρ is the solution density, v the sound velocity, α_P the coefficient of thermal expansion, C_p the specific heat, and Γ the concentration dependence ($\Gamma^{-1} = [LS]^{-1} + [HS]^{-1}$ where [LS] and [HS] are the concentrations of the singlet and quintet isomers, respectively); ΔV° and ΔH° are the volume and enthalpy differences between the two isomers, respectively. Values of ΔH° and Γ are obtained from the determination of the equilibrium constant by the NMR method. The other quantities are taken from the literature.[16,24] These are listed in Tables I and II, together with the values of ΔV° calculated using eq 4 from the experimental results at three different temperatures.

An average of 22 ± 1 $cm^3\ mol^{-1}$ is obtained for the volume difference between the low-spin and high-spin isomers of $Fe(HB(pz)_3)_2$. The small trend with temperature is probably not a real effect but the result of the accumulation of most of the experimental errors. Although no crystal structure information is available for the iron(II) complex, a single-crystal x-ray structure determination of the analogous $Co(HB(pz)_3)_2$ is available.[25] From these data one calculates that the effective radius from the central metal to the peripheral hydrogen atoms on the pyrazole rings is approximately 6 Å. If 6.00 Å is used as the radius of a sphere describing the low-spin state, then the measured volume change of 22 $cm^3\ mol^{-1}$ corresponds to a radial extension of 0.08 Å on passing to the larger high-spin state. This can be considered a minimum change in metal-ligand distance between the low-spin and high-spin isomers, since examination of the crystal structure or of molecular models reveals that the surface of the complex is deeply indented with space between the planes of the pyrazole groups. The volume change due to an extension of the metal-ligand bond is much less for this dimpled surface than for a sphere. Hence the measured ΔV° probably corresponds to a 0.10-0.15-Å change in the metal-ligand bond length.

Similarly, the volume difference between the high-spin and low-spin isomers of $Fe(papth)_2^{2+}$ is found to be 11.0 ± 0.3 $cm^3\ mol^{-1}$. No crystal structure information appears to be available on salts of this complex. This volume difference again appears to be of a reasonable magnitude for such a spin equilibrium between the low-spin $(t_{2g})^6$ and high-spin $(t_{2g})^4(e_g^*)^2$ electron configurations, based on accumulating crystallographic evidence[26] on the structural effects of antibonding e_g^* electrons.

The ultrasonic relaxation amplitudes are thus consistent with our assignment of the absorption to the spin-equilibrium relaxation.

The rate constants for the intersystem crossing between spin states can be calculated from the relaxation times. For a unimolecular isomerization reaction between the low-spin singlet state and the high-spin quintet state

$$\tau^{-1} = k_{15} + k_{51} = k_{51}(K_{15} + 1) \qquad (5)$$

Using the equilibrium constants determined by the NMR method, the rate constants given in Tables I and II are obtained.

The most significant aspect of these results is the temperature dependence of the rate constants (Figures 6 and 7). The free-energy barriers calculated from the rate constants at 25 °C and the activation parameters obtained from their temperature dependence using absolute rate theory, eq 6, are given in Tables I and II and illustrated in Figures 8 and 9.

$$k = \left(\frac{k_B T}{h}\right)e^{-\Delta G^\ddagger_{obsd}/RT} = \left(\frac{k_B T}{h}\right)e^{-\Delta H^\ddagger_{obsd}/RT}e^{\Delta S^\ddagger_{obsd}/R}$$
$$= \kappa\left(\frac{k_B T}{h}\right)e^{-\Delta H^\ddagger_{obsd}/RT}e^{\Delta S^\ddagger/R} \qquad (6)$$

From these results an assessment can be made of the magnitude of κ, the transmission coefficient which reflects the probability of the spin-forbidden intersystem crossing. This will be done for the two complexes in turn.

For $Fe(HB(pz)_3)_2$ the rate constants k_{15} of $4.93 \times 10^6\ s^{-1}$ and k_{51} of $2.53 \times 10^7\ s^{-1}$ at 25 °C correspond to activation free energies $\Delta G^\ddagger_{15}$ of 8.32 kcal mol^{-1} and $\Delta G^\ddagger_{51}$ of 7.36 kcal mol^{-1}. The difference of 0.96 kcal mol^{-1} is of course ΔG°_{15}. For the singlet-quintet process the activation enthalpy $\Delta H^\ddagger_{15}$ is 5.64 kcal mol^{-1} but this comprises 5.03 kcal mol^{-1} due to the endothermic enthalpy difference ΔH°_{15}. For the reverse quintet-singlet process the activation enthalpy $\Delta H^\ddagger_{51}$ is therefore only 0.62 kcal mol^{-1}. Hence the rate constant k_{51} is determined largely by an entropic barrier equivalent to $-T\Delta S^\ddagger_{obds}$ of 6.74 kcal mol^{-1}. This temperature-independent contribution to the free energy barrier comprises both κ and other entropy terms so that the relative magnitudes of these two factors cannot be separated experimentally. To estimate κ requires an additional assumption.

A minimum value of κ and hence the lowest probability of intersystem crossing is obtained by assuming that the entropy of the transition state equals that of the high-spin quintet state.

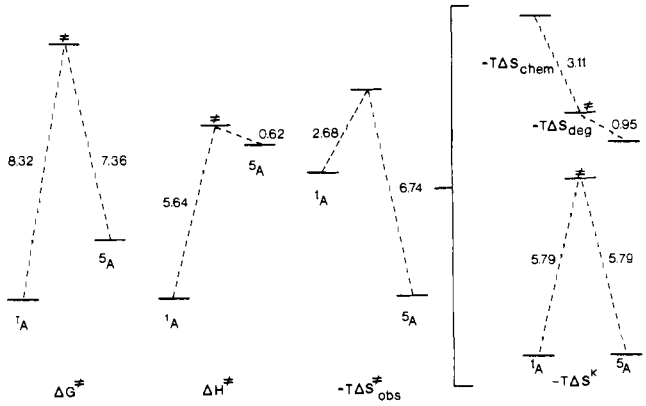

Figure 8. Activation parameters for $Fe(HB(pz)_3)_2$ obtained from absolute rate theory, with $-T\Delta S^{\neq}_{obsd}$ partitioned to give the minimum value of κ as described in the text.

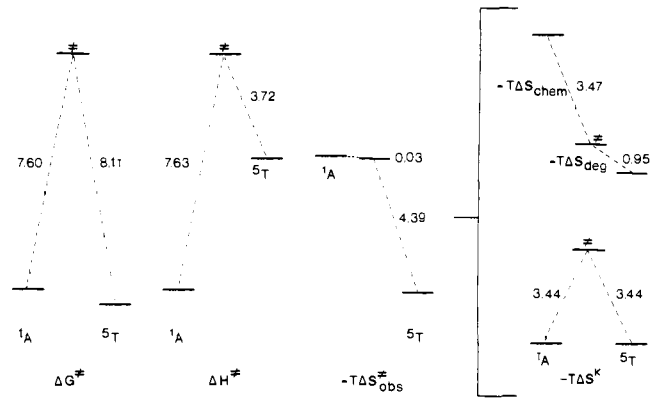

Figure 9. Activation parameters for $Fe(papth)_2^{2+}$ obtained from absolute rate theory, with $-T\Delta S^{\neq}_{obsd}$ partitioned to give the minimum value of κ as described in the text.

Then the entire entropic barrier for the quintet-singlet process of 6.74 kcal mol^{-1} is due to κ, which has the value $10^{-4.9}$. This estimate of a minimum value of κ involves the additional assumption that the entropy of the transition state is not greater than that of the quintet isomer, i.e., that there is no minimum in $-T\Delta S^{\ddagger}$ between the quintet and singlet states. This assumption must be valid in the present case, since the enthalpy barrier of 0.62 kcal mol^{-1} is equal to the thermal energy at room temperature. Were there a minimum in $-T\Delta S^{\ddagger}$ lower than the quintet state, the quintet state would be found in that potential well.

Consideration of the spin degeneracy leads to a more realistic lower limit for κ. The quintet state possesses higher entropy due to its fivefold spin degeneracy equal to a free-energy stability of 0.95 kcal mol^{-1} at 25 °C. This assumes that the threefold orbital degeneracy has been lifted so that the ground state is ^{5}A, as occurs in the closely related methylpyrazole complex in the solid state.[27] In the transition from singlet to quintet the complex acquires this additional entropy but this presumably must occur after passage from the singlet state. This implies by microscopic reversibility that for the quintet to singlet process only one of the five microstates is reactive—presumably the one with $m_s = 0$—and hence that the quintet state must lose entropy equivalent to the spin degeneracy to reach the transition state. This contribution imposes a minimum entropy barrier equivalent to 0.95 kcal mol^{-1} and hence reduces the minimum probability for intersystem crossing, κ, to $10^{-4.2}$.

For $Fe(papth)_2^{2+}$ a similar analysis leads to a larger value for κ, since for this complex there are appreciable enthalpies of activation for the intersystem crossing in both directions (Figure 9). This means that the absence of a minimum in $-T\Delta S^{\ddagger}$ is not required thermodynamically, but we believe this restriction on the transition state entropy to be reasonable considering the nature of the isomerization process. With this assumption, and considering the spin degeneracy as above but ignoring any further contribution from orbital degeneracy, a minimum value for κ of $10^{-2.5}$ is obtained.

The transmission coefficient κ can be interpreted in terms of the interaction energy between two potential energy surfaces at the crossing point (Figure 10) using the Landau-Zener model. A value of $\kappa \ll 1$ implies that the system is highly nonadiabatic, with the reactant infrequently crossing onto the product potential energy surface; i.e., instead of remaining on the lower solid curve in Figure 10, it follows the dotted line onto the upper energy surface. If the energy separation between the upper and lower surfaces increases, the reaction becomes more adiabatic, κ becomes larger, and the system stays on the lower surface more frequently. With the assumption that both surfaces can be represented by identical harmonic oscillators with

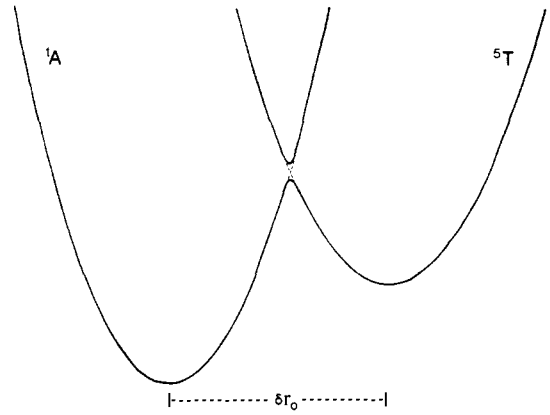

Figure 10. Illustration of the potential energy surfaces showing the difference in metal-ligand bond lengths and the nonadiabatic intersystem crossing process (lower surface).

a fundamental frequency of 300 cm^{-1} and reduced mass of 50, separated by 0.10 Å, a transmission coefficient $\kappa > 10^{-3}$ implies an energy separation greater than 12 cm^{-1}. While this value has no quantitative significance, it appears to be of a reasonable order of magnitude.

This result is more significant, however, when the recent theoretical results of König and Kremer are considered.[29] These authors have shown that, among the possible spin-equilibrium situations arising from either octahedral or tetrahedral d^4, d^5, d^6, or d^7 electron configurations, only for the present octahedral d^6 case is there no substantial mixing between the two states at the crossover point. We interpret this to mean that the splitting of the order of 12 cm^{-1} derived from our relaxation measurements is a small value arising from higher order effects not considered in their theory, and that for other electron configurations the splitting is substantially larger. This implies that for these other electron configurations the transmission coefficient κ will be much larger.

These arguments suggest an important hypothesis regarding the dynamics of intersystem in metal complexes: only for octahedral d^6 complexes can the transmission coefficient be significantly less than unity. In the absence of additional, e.g., steric, barriers to isomerization, the rates of intersystem crossing in d^6 complexes are determined by κ and the thermodynamic differences between the isomers. For other electron configurations without additional activation barriers the rates are determined by the thermodynamic factors alone since κ may approach unity. This may explain the apparently very rapid relaxation of some cobalt(II) and iron(III) complexes. We observe no excess ultrasonic absorption for solutions of

bis(terpyridine)cobalt(II) ion or tris(diethyldithiocarbamato)iron(III), even though spin equilibria in solution are well documented in each case.[1,4,30,31] If $\kappa \sim 1$ the rate constants could be greater than 10^{10} s^{-1}, since the thermodynamic barriers are small. Because the excess ultrasonic absorption depends linearly on τ (eq 4), a process with such a short relaxation time would not display a measurable relaxation amplitude. This hypothesis requires, however, that those complexes of d^4, d^5, and d^7 electron configurations which do exhibit spin-equilibrium relaxation with rate constants in the range 10^6-10^8 s^{-1} should possess activation energy barriers in addition to those imposed by ground-state thermodynamic differences. Measurements are in progress to test this hypothesis.

In conclusion, we have determined the rates of two $\Delta S = 2$ intersystem crossing processes by measuring the ultrasonic relaxation of the thermal spin equilibria in solution. Within the framework of absolute rate theory, this establishes lower limits for the transmission coefficients κ, which are a measure of the adiabaticity of the surface crossing. We must note that the systems studied are thermally equilibrated, without the necessity for large energy transfers as may be found in excited state processes. Finally, we emphasize that for transition metal complexes spin state changes are generally accompanied by substantial coordination geometry rearrangements due to the change in electron population of antibonding orbitals. It is these, rather than purely electronic effects, which may determine the rates of most "spin-state" isomerization reactions.

Acknowledgments. We gratefully acknowledge the generous cooperation of Professor S. Petrucci, Polytechnic Institute of Brooklyn, in performing an initial ultrasonic relaxation experiment which encouraged us to proceed with this work. We thank Professor H. Pollard, Dr. J. Dunlop, and Mr. M. Benton, Department of Physics, University of New South Wales, for providing access to the Arenberg electronics necessary for our first pulsed experiments and for the hospitality of their laboratory, Mr. Peter Watson for skilled machine work, Dr. H. A. Goodwin, University of New South Wales, for the sample of $[Fe(papth)_2]Cl_2 \cdot 2H_2O$, Professor N. S. Hush, Sydney University, and Professor T. J. Meyer, University of North Carolina, for helpful discussions, and Professor L. J. Wilson, Rice University, and Dr. N. Sutin, Brookhaven National Laboratory, for useful correspondence. This research was supported in part by the Australian Research Grants Committee and in part by the donors of the Petroleum Research fund, administered by the American Chemical Society. The new Arenberg pulsed ultrasonic electronics was acquired through a grant from the Sydney County Council.

References and Notes

(1) R. L. Martin and A. H. White, *Transition Metal Chem.*, **5**, 113 (1969).
(2) M. Kasha, *Discuss. Faraday Soc.*, **9**, 14 (1950); V. Balzani and V. Carassiti, "Photochemistry of Coordination Compounds", Academic Press, New York, N.Y., 1970.
(3) M. A. Hoselton, L. J. Wilson, and R. S. Drago, *J. Am. Chem. Soc.*, **97**, 1722 (1975), and references cited therein.
(4) J. K. Beattie, N. Sutin, D. H. Turner, and G. W. Flynn, *J. Am. Chem. Soc.*, **95**, 2052 (1973).
(5) M. F. Tweedle and L. J. Wilson, *J. Am. Chem. Soc.*, **98**, 4824 (1976).
(6) S. Trofimenko, *J. Am. Chem. Soc.*, **89**, 3170 (1967).
(7) D. F. Evans, *J. Chem. Soc.*, 2003 (1959); T. H. Crawford and J. Swanson, *J. Chem. Educ.*, **48**, 382 (1971).
(8) A. L. van Geet, *Anal. Chem.*, **42**, 679 (1970).
(9) M. L. Kaplan, F. A. Bovey, and H. N. Cheng, *Anal. Chem.*, **47**, 1703 (1975).
(10) F. Eggers, *Acustica*, **19**, 323 (1967–1968); F. Eggers and Th. Funck, *Rev. Sci. Instrum.*, **44**, 969 (1973).
(11) A. Labhardt and G. Schwarz, *Ber. Bunsenges. Phys. Chem.*, **80**, 83 (1976).
(12) National Measurements Laboratory, CSIRO, Sydney, Australia.
(13) Dow-Corning RTV 732 is used for water and polar organic solvents; RTV 733 is used for nonpolar aromatic solvents.
(14) J. H. Andreae, R. Bass, E. L. Heasell, and J. Lamb, *Acustica*, **8**, 131 (1958); G. Atkinson, S. K. Kor, and R. L. Jones, *Rev. Sci. Instrum.*, **35**, 1270 (1964); J. H. Andreae and P. L. Joyce, *Br. J. Appl. Phys.*, **13**, 462 (1962).
(15) L. G. Jackopin and E. Yeager, *J. Phys. Chem.*, **74**, 3766 (1970).
(16) P. Jagodzinski and S. Petrucci, *J. Phys. Chem.*, **78**, 917 (1974).
(17) J. Steuhr, T. Noveske, and D. F. Evans, *J. Phys. Chem.*, **77**, 912 (1973).
(18) J. Steuhr in "Techniques of Chemistry", Vol. VI, Part II, 3rd ed, A. Weissberger, Ed., "Investigation of Rates and Mechanisms of Reactions", G. G. Hammes, Ed., Wiley-Interscience, New York, N.Y., 1974, p 237.
(19) J. P. Jesson, S. Trofimenko, and D. R. Eaton, *J. Am. Chem. Soc.*, **89**, 3158 (1967).
(20) J. Fleisch, P. Gütlich, and K. M. Hasselbach, *Inorg. Chem.*, **16**, 1979 (1977); E. König, G. Ritter, W. Irler, and B. Kanellakopulos, *J. Phys. C*, **10**, 603 (1977); J. Fleisch, P. Gütlich, K. M. Hasselbach, and W. Müller, *Inorg. Chem.*, **15**, 958 (1976).
(21) R. N. Sylva and H. A. Goodwin, *Aust. J. Chem.*, **20**, 479 (1967).
(22) E. König, G. Ritter, and H. A. Goodwin, *Chem. Phys. Lett.*, **44**, 100 (1976).
(23) C. M. Harris and E. Sinn, *Inorg. Chim. Acta*, **2**, 296 (1968); H. A. Goodwin and D. W. Mather, *Aust. J. Chem.*, **25**, 715 (1972).
(24) J. A. Riddick and W. B. Bunger in "Techniques of Chemistry", Vol. II, 3rd ed, A. Weissberger, "Organic Solvents", Wiley-Interscience, New York, N.Y., 1970, p 220.
(25) M. R. Churchill, K. Gold, and C. E. Maw, Jr., *Inorg. Chem.*, **9**, 1597 (1970).
(26) E. König and K. J. Watson, *Chem. Phys. Lett.*, **6**, 457 (1970); B. F. Hoskins and C. D. Pannan, *Inorg. Nucl. Chem. Lett.*, **11**, 409 (1975); J. G. Leipoldt and P. Coppens, *Inorg. Chem.*, **12**, 2269 (1973).
(27) J. P. Jesson, J. F. Weiher, and S. Trofimenko, *J. Chem. Phys.*, **48**, 2058 (1968).
(28) W. Kauzmann, "Quantum Chemistry", Academic Press, New York, N.Y., 1957, p 541.
(29) E. König and S. Kremer, *Theor. Chim. Acta*, **26**, 311 (1972); *Ber. Bunsenges. Phys. Chem.*, **78**, 786 (1974), and references cited therein.
(30) J. G. Schmidt, W. S. Brey, Jr., and R. C. Stoufer, *Inorg. Chem.*, **6**, 268 (1967).
(31) G. R. Hall and D. N. Hendrickson, *Inorg. Chem.*, **15**, 607 (1976).